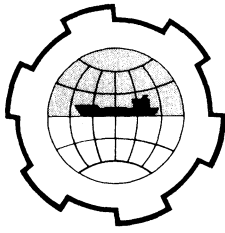


PORT AND OCEAN ENGINEERING UNDER ARCTIC CONDITIONS
TECHNICAL UNIVERSITY OF NORWAY



PREVENTION OF ICE FORMATION BY FORCED MIXING

Torkild CARSTENS
Assoc. Professor

River and Harbour Lab.
Techn. Univ. of Norway

Trondheim
Norway

ABSTRACT

In order to prevent the Rana Fjord from freezing due to increased winter inflow of fresh water from hydro power storage reservoirs, an air bubbler was installed at the mouth of the Rana River in 1968.

Three seasons of successful operation have since proven the feasibility of this method of forced mixing under the given set of oceanographical and meteorological conditions.

The mechanics of the mixing process are discussed in the light of observations made partly in experiments prior to construction, partly in situ after completion of the air bubbler.

PREVENTION OF ICE FORMATION BY FORCED MIXING

THE PROBLEM

In many of the Norwegian fjords the natural stratification is disturbed by extensive hydro-power developments, because the construction of artificial storage reservoirs interferes with the natural inflow of fresh water. The purpose of the artificial storage is to make the runoff hydrograph conform more to the power load curve. In a Northern climate this means holding back summer flows in order to increase the winter discharge. For instance, in the Rana River, winter flows are increased 2-3 times.

Any increase of the winter inflow will increase the ice hazard in a fjord. Experience from Sørfjorden, the Southern branch of the Rana Fjord, shows that an ice cover is likely to form unless the river water is mixed with the fjord water. For this purpose a gigantic mixer was designed for the Rana River and put into operation in December 1969.

Cooling and freezing of sea water

Provided there are no heat gains, the heat loss a water surface can suffer before freezing is proportional to the temperature difference ΔT

$$\begin{aligned}\Delta T &= T_v - T & S < 24.70/00 \\ \Delta T &= T_g - T & S > 24.70/00\end{aligned}\quad (1)$$

where $T_v(S)$ is the temperature of maximum density, $T_g(S)$ the freezing point and T the bulk temperature of the surface layer (Fig. 2). Of course there is no freezing before $T = T_g$, however, for $S < 24.70/00$ there is no free convection. In the absence of turbulence a surface film would then rapidly reach the freezing point.

The stable stratification that develops during cooling for $S < 24.70/00$ and stops the free convection also hampers turbulent mixing. Fig. 3 shows that the strongest cooling stability occurs for $S = 5-10/00$, a salinity range commonly encountered at heads of fjords.

Compared with the prevailing salinity stratification the temperature stratification is insignificant for the static stability of the water column in those of our fjords that are threatened by ice. The so-called winter circulation induced by cooling for $S > 24.70/00$ does not materialize because of the vertical salinity gradient. On the other hand there is always some turbulent mixing. During the dark winter at higher latitudes ice-free waters are maintained exclusively by turbulent transport of heat and salt water to the surface and of fresh water away from it.

The wind shear at the water surface and the shear stresses caused by velocity gradients within the water mass are the natural turbulence-generating inputs. The inflow of fresh water has a predominating influence on the stability and is the turbulence-damping input.

If for some reason the fresh water inflow is increased, the frequency of ice cover formation will increase. This can be avoided only by a corresponding increase of the turbulence, since we have no practical technology for heat loss control from a large water surface. The answer to increased winter inflow of fresh water, if more ice is not acceptable, is forced mixing.

THE AIR BUBBLER

Forced mixing requires two forms of kinetic energy supply to the water masses one wants to mix:

- i) In order to bring the water masses together, they must be given a mean velocity towards the mixing zone,
- ii) For the actual mixing a sufficient turbulence must be present in the mixing zone.

Using compressed air for the transfer of energy to the water, both these tasks were accomplished by one single, and mechanically very simple, submerged installation.

At a depth of 15 m two perforated, parallel pipes were suspended across the mouth of the Rana River. (Fig. 1). That part of the river mouth which was too shallow, was closed by a jetty, constricting the total width to about 400 m.

The fresh water normally flows into the fjord as a surface jet at velocities up to 65 cm/s at falling tide, and salinities less than

100/00, for the design discharge of $Q_f = 200 \text{ m}^3/\text{s}$.

It was felt that by increasing the average salinity in the surface layer to $S = 250/00$, the reduced vertical stability would allow a sufficient further mixing by natural processes to prevent freezing.

The sea water barrier

The vertical flow generated by the released air sets up a stagnation hump on the water surface. In still water this hump is symmetrical and provides the necessary pressure gradients to deflect the vertical flow into two horizontal ones. In order to arrest a flowing surface layer, the height of the hump should equal or exceed the velocity head $\frac{v^2}{2g}$ of this layer. The salt water then forms an effective barrier, a dam as it were, across the river mouth. The river flow must pass through this barrier, and in the process it is mixed with sea water.

Compressor capacity

BULSON (1961) gives a formula for the horizontal surface velocity generated by air released in homogeneous water.

$$v_m = 1,46(gq_a)^{1/3} \left(1 + \frac{D}{H_0}\right)^{-1/3} \quad (2)$$

$$h = 0,32 H_0 \ln\left(1 + \frac{D}{H_0}\right) \quad (3)$$

g - gravitational acceleration

$q_a = \frac{Q_a}{L}$ air discharge per unit length

D - depth of pipe

H_0 - atmospheric pressure in m of water

h - thickness of surface current

Field tests carried out in the Rana Fjord in 1962 (BERGE 1965) showed that (2) could be used to estimate the necessary power to break through the surface layer with a vertical sea water jet, simply by requiring

$$v_m \geq v \quad (4)$$

Further tests carried out in the harbour of Trondheim in 1967 (RHL, unpublished report) confirmed the favourable 1962 results with two rather than one single air pipe.

By distributing the air flux along two parallel pipes a significant gain in efficiency is obtained. Visual observations of the surface show two maxima in the distribution of air bubbles across the pipe when the air flux and the submergence is low (low tide, near shore). For high air fluxes the two parallel rising jets merge into one single jet.

Unless the one-peaked jet caused by merger of two jets concentrates the air bubbles better than the jet from a single air pipe it is difficult to understand why the horizontal surface velocities caused by the former jet exceed those of the latter. The merging of bubble plumes has been visually studied at RHL on a small scale. Recently LISETH 1970 has reported interesting results of tests with merging buoyant jets that are much less diluted than single jets.

Based on a maximum velocity $v = 65$ cm/s the air discharge was determined by (2), (3) and (4). Two compressors, each delivering $150 \text{ m}^3/\text{min}$ at 3 kp/cm^2 , were installed.

PERFORMANCE TEST

In April 1969, after the first season of successful operation, an attempt was made to measure the flows generated by the air bubbler.

Current speed and direction, temperature and salinity were gauged every two hours during one tidal period, with constant air discharge. The upstream source of the fresh water discharge, the Rana power plant, maintained an almost constant release rate. However, because of the 2,5 m tidal range the surface layer discharge at the gauged sections varied considerably.

Eight gauging stations were used, four in section 1 upstream and four in section 2 downstream of the air bubbler. For each station about 10 point measurements were made.

The basic data are given in Tables 1 and 2 below. Tables 3 and 4 convey an idea of the performance of the air bubbler, and the data of Table 5 give a gross picture of its fluid mechanics.

Volume flux. In row 2 of Table 3 the entrained volume flux $Q_2 - Q_1$ is compared with Q_B given by (2) and (3). The entrainment is from 28-62% of the horizontal flow set up by the same air flux released in stagnant, homogeneous water. When compared with the upstream discharge, Q_1 , the entrained flow ranged from 42% to about 500%.

It is apparent that no predictions of entrainment in a two-layer system can be based on volumetric flow rates generated in homogeneous water.

Salinity increase. As intended, the salinity of the surface layer (Table 2) is raised well above the intersection of $T_v(S)$ and $T_g(S)$ at $S = 24,7$ o/oo in Fig. 2. The salinity change across the air bubbler $S_2 - S_1$ is compared with the vertical difference $S_{15} - S_1$ in row 1 of Table 4. S_{15} varies between 30 and 34 o/oo, so a considerable depression of the freezing point in the surface layer is feasible.

Temperature increase. The observed temperature increase corresponds well with the observed salinity increase (Table 4).

There is always a vast heat reservoir in the fjord, with T_{15} around 5°C .

Cooling capacity. The cooling capacities ΔT of nonturbulent water given by (1) are shown in table 3. While cold weather would reduce ΔT_1 to zero, ΔT_2 would be little influenced, as indicated by the high values of rows 2 and 3 of Table 4.

Stability. A further measure of the extent to which the stratification has been broken down is given by the stability ratios of row 6 in Table 4. The stability E of a water column is described by

$$E = \frac{1}{\rho} \frac{d\rho}{dz} = \frac{1}{\rho} \frac{d\rho}{dS} \frac{dS}{dz} \quad (5)$$

Approximating $\frac{dS}{dz}$ by its layer mean $\frac{\Delta S}{\Delta z}$, the stability reduction is indicated by the ratio

$$\frac{E_2}{E_1} = \frac{S_{15}-S_2}{S_{15}-S_1} \frac{h_1}{h_2} \quad (6)$$

It should be noted that the downstream surface layer is still stable, with E_2 ranging from $0.6 \cdot 10^{-3}$ to $0.6 \cdot 10^{-4} \text{ m}^{-1}$. These stabilities are sufficient to prevent free convection during cooling. The fact that freezing has not yet occurred with the air bubbler operating, points to turbulent transport of heat to the surface as an all-important mechanism in preventing freezing.

Entrainment and diffusion. The data of Table 1 permit estimates of entrainment and diffusion fluxes of salt and heat into the surface layer.

The entrainment of salt is given by

$$Q_{eS} = (Q_2 - Q_1) S_{15} \quad (7)$$

and of heat by

$$Q_{eT} = (Q_2 - Q_1) T_{15} \quad (8)$$

These estimates are probably high, because it is unlikely that the entrained fluxes should come from depths lower than the air pipe itself.

The diffusion of salt is given by

$$Q_{dS} = Q_2 S_2 - Q_1 S_1 - (Q_2 - Q_1) S_{15} \quad (9)$$

and of heat by

$$Q_{dT} = Q_2 T_2 - Q_1 T_1 - (Q_2 - Q_1) T_{15} \quad (10)$$

The ratio $(\frac{Q_d}{Q_e S})$ for salt checks well with the same ratio $(\frac{Q_d}{Q_e T})$ for heat (rows 6 and 7, Table 5).

Within the range covered by the tests the diffusion flux averages about 9% of the entrainment flux as estimated by the present method.

CONCLUSIONS

The air bubbler mixes fresh water with sea water almost exclusively by entrainment. Of the heat and salt mixed into the overcurrent entrainment accounted for 11 times more than diffusion. This means that 91% of the fresh water remained in the overcurrent and was diluted there, while 9% was removed and mixed into deeper layers.

The temperature and salinity in the overcurrent can be raised to better than 95% of the prevailing temperature and salinity at the depth of the air pipe.

The average static stability $E = \frac{1}{\rho} dp/dz$ of the pycnocline separating the overcurrent from the fjord underneath can be reduced from $E = 10^{-2}$ to 10^{-4} . This is not sufficient to induce thermal convection (winter circulation). However, the reduced stability seems to allow the prevailing turbulence to maintain the vertical transports of heat and salt necessary to prevent freezing.

REFERENCES

- BERGE, H. 1965: Prevention of ice formation in estuaries by mixing of salt and fresh water - XI Congress IAHR, Leningrad.
- BULSON, P.S. 1961: Currents Produced by an Air Curtain in Deep Water. The Dock & Harbour Authority - May 1961.
- LISETH, P. 1970: Mixing of merging buoyant jets. HEL 23-1 University of California, Berkeley
- TRÆTTEBERG, A 1967: Bubble curtain by air release from parallel pipes. Internal report, RHL, 600185.

Table 1 Observed fluxes

Test	Q_a	Q_f	Q_1	$Q_1 S_1$	$Q_1 T_1$	Q_2	$Q_2 S_2$	$Q_2 T_2$
1	75	85-90	99,5	1,290	407,2	274,7	7,629	1432,4
2	112	90-95	111,4	1,007	389,5	314,1	8,493	1628,7
3	150	80-85	109,3	1,338	415,5	401,6	12,310	2167,6
4	300	75-80	74,3 ^{x)}	0,864	329,4	577,5	18,765	3142,1

^{x)} doubtful, 90 m³/s is more likely

Table 2 Other observed parameters

Test	h_1	S_1	T_1	h_2	S_2	T_2	S_{15}	T_{15}
1	1,25	13,0	4,0	4,9	27,8	5,2	33,7	5,7
2	1,3	9,0	3,5	5,3	27,0	5,2	33,8	5,6
3	1,65	12,2	3,8	6,9	30,7	5,4	33,8	5,5
4	1,5	9,6	3,7	13,2	32,5	5,4	33,7	5,4

Table 3 Some performance characteristics

Test	$\frac{Q_2 - Q_1}{Q_B}$	$\frac{Q_2 - Q_1}{Q_1}$	$T_v(S_1)$	$T_g(S_2)$	ΔT_1	ΔT_2
1	0,28	1,76	1,3	- 1,5	2,8	6,7
2	0,36	1,82	2,1	- 1,5	1,4	6,7
3	0,50	2,67	1,4	- 1,7	2,4	7,1
4	0,62	5,41	1,9	- 1,8	1,8	7,2

Table 4 Stratification and stability

Test	$\frac{S_2 - S_1}{S_{15} - S_1}$	$\frac{T_2 - T_1}{T_{15} - T_1}$	E_1	E_2	E_2/E_1
1	0,71	0,69	$33,1 \cdot 10^{-3}$	$2,409 \cdot 10^{-3}$	0,072
2	0,73	0,81	$38,2 \cdot 10^{-3}$	2,567	0,067
3	0,86	0,94	$26,2 \cdot 10^{-3}$	0,900	0,034
4	0,95	1,00	$32,2 \cdot 10^{-3}$	0,182	0,006

Table 5 The mixing mechanisms

Test	Q_{eS}	Q_{eT}	Q_{dS}	Q_{dT}	$\left(\frac{Q_d}{Q_e}\right)_S$	$\left(\frac{Q_d}{Q_e}\right)_T$
1	5,904	998,64	0,435	40,0	0,074	0,040
2	6,851	1135,12	0,635	104,08	0,093	0,092
3	9,880	1607,65	1,092	144,45	0,111	0,090
4	16,429	2632,50	1,472	180,20	0,090	0,068

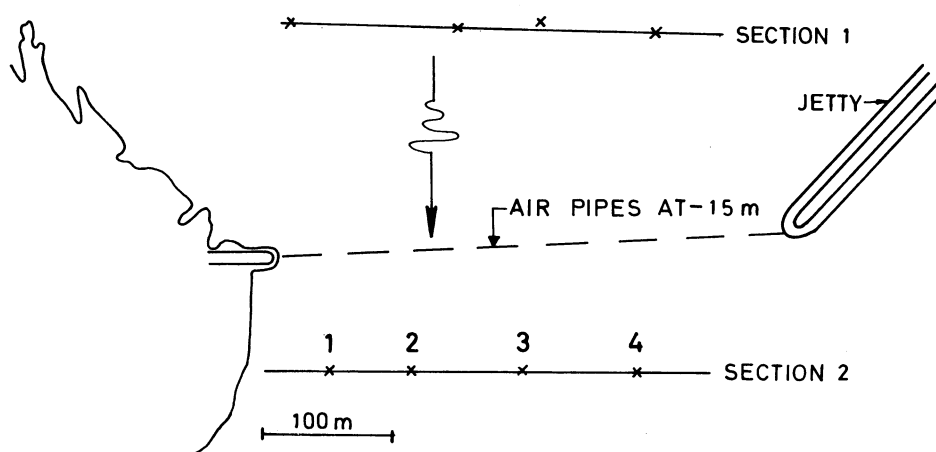


Fig. 1. THE RANA AIR BUBBLER

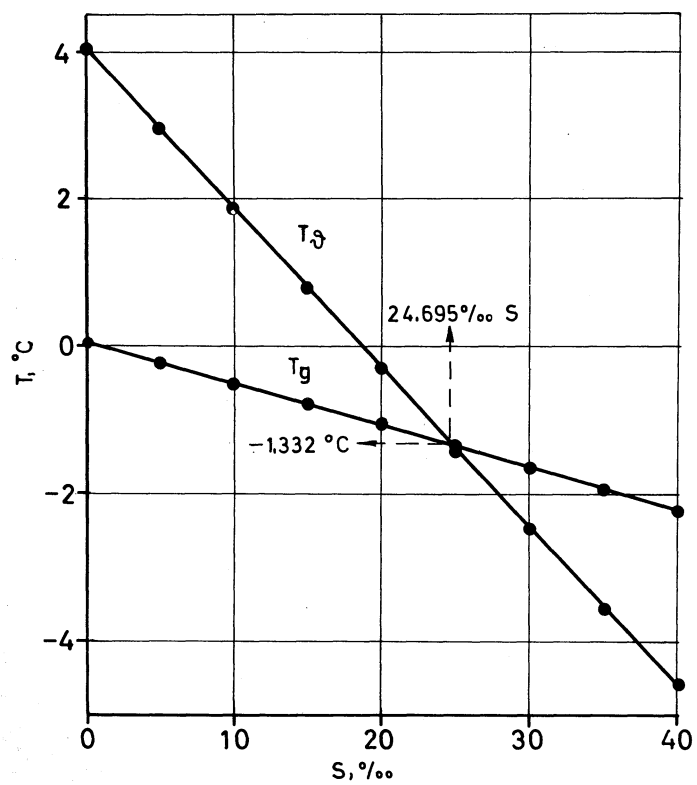


Fig. 2. Dependence of freezing temperature T_g and temperature of maximum density T_ρ on the salinity S

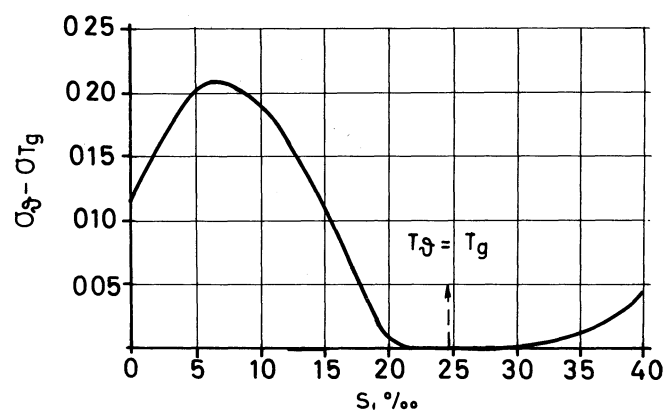


Fig. 3. Difference $\sigma_\rho - \sigma_{T_g}$ between maximum density and density at the freezing point as a function of salinity S